P H Y S I C A L   R E V I E W   L E T T E R S

Spin-Orbit Hybridization Points in the Face-Centered-Cubic Cobalt Band Structure

M. Pickel,[1,2] A. B. Schmidt,[1,2] F. Giesen,[2] J. Braun,[1,3] J. Minár,[3] H. Ebert,[3] M. Donath,[1] and M. Weinelt[2,4,*]

[1]*Physikalisches Institut, Westfälische Wilhelms-Universität Münster, Wilhelm-Klemm-Straße 10, 48149 Münster, Germany*
[2]*Max-Born-Institut, Max-Born-Straße 2A, 12489 Berlin, Germany*
[3]*Department Chemie und Biochemie, Physikalische Chemie, Ludwig-Maximilians Universität München, 81377 München, Germany*
[4]*Freie Universität Berlin, Fachbereich Physik, Arnimallee 14, 14195 Berlin, Germany*

Linear magnetic dichroism is observed in spin-, time-, and energy-resolved two-photon photoemission from valence bands of epitaxial fcc cobalt on Cu(001). With image-potential states as spectator states we identify initial bulk and surface states with minority spin character as the source for dichroic intensities and apparent dichroic lifetimes. Excellent agreement with *ab initio* fully relativistic calculations of the cobalt fcc band structure allows us to precisely determine spin-orbit hybridization points close to the Fermi level. These spin hot spots enhance spin-flip scattering by several orders of magnitude and are therefore assumed to be crucial in ultrafast demagnetization.

The spin-orbit interaction couples the electron's spin and magnetic moment to the crystal lattice. It thereby governs important properties of ferromagnetic materials such as the magneto-crystalline anisotropy, magnetostriction, and the anisotropy of the magnetoresistance [1,2]. Furthermore, spin-orbit coupling is responsible for the transfer of angular momentum from the spin system to the lattice upon reversal of the magnetization, long-known from the Einstein–de Haas effect. For the itinerant ferromagnets this process is believed to occur on the time scale of the ensemble-averaged spin-lattice relaxation time of some picoseconds [3,4]. This time scale constitutes an as yet unresolved bottleneck for the loss of the spin-magnetic moment on a *femtosecond* time scale in optically driven demagnetization [4,5]. In recent model calculations it was shown that with Elliot-Yafet type electron-phonon scattering, i.e., scattering between spin-orbit coupled electronic states, femtosecond demagnetization can be explained [6]. However, the spin-flip probability per scattering event ($\propto Z^4$) was assumed to be about 2 orders of magnitude higher than a value extrapolated from nonmagnetic metals of similar atomic number Z. In purely nonrelativistic electron-electron or electron-phonon scattering such a spin flip is not possible because the Coulomb operator does not act on the spin part of the electron wave function. Only in the presence of spin-orbit coupling can electrons undergo a spin flip and thus cause a net demagnetization [7]. The spin-flip scattering probability increases significantly at hybridization points in the band structure. These so called spin hot spots have been identified in *ab initio* calculations to overcome the discrepancy between measured spin-lattice relaxation rates in aluminum and the much lower estimate based on atomic properties [8]. Avoided crossing and concomitant spin mixing of bands close to the Fermi level E_F can likewise explain optically driven ultrafast demagnetization in the $3d$ ferromagnets [9], since excited electrons or holes relax towards the

Fermi level in the first hundred femtoseconds of carrier thermalization via inelastic electron-electron scattering.

In this Letter we identify hybridization points in the valence band structure of ferromagnetic fcc cobalt films on Cu(001). The observation of magnetic linear dichroism (MLD) in two-photon photoemission (2PPE) is used to extract the spin-orbit coupling along the Δ direction. In time- and energy-resolved measurements both the photo-electron current and the apparent lifetime of image-potential states (IPS) depend on the magnetization direction. We find in spin-resolved measurements that this MLD is dominated by hybridization of bulk and surface valence bands with spin-minority character. In contrast to conventional photoemission, where a (dichroic) background renders the determination of exact energetic positions difficult, 2PPE is virtually background free. Therefore the experimental data allow us to precisely determine the position of hybridization points close to the Fermi level and the spin-orbit splitting. These values serve as benchmarks for a fully relativistic multiple-scattering calculation of the cobalt band structure. The calculation reveals an additional spin hot-spot along the Σ direction of the fcc Brillouin zone with the energy strongly determined by electronic correlations.

The 2PPE experiment is sketched in Fig. 1(a) [10]. We use the frequency-tripled ($3h\nu$) output of a mode-locked, tunable Ti:sapphire laser to excite electrons from occupied bulk or surface states at initial-state energy $E_i = E - E_F$ into the unoccupied IPS at energy E_n, $n = 1, 2, \ldots$ [11]. From these intermediate states electrons are lifted above the vacuum level E_{vac} by the laser fundamental ($h\nu$). The kinetic energy E_{kin} is analyzed in a cylindrical sector analyzer and the spin polarization is determined by spin-polarized low-energy electron diffraction [12]. Six and seven monolayers (ML) cobalt are evaporated on cleaned Cu(001) held at 90 K and subsequently annealed to 490 K [13].
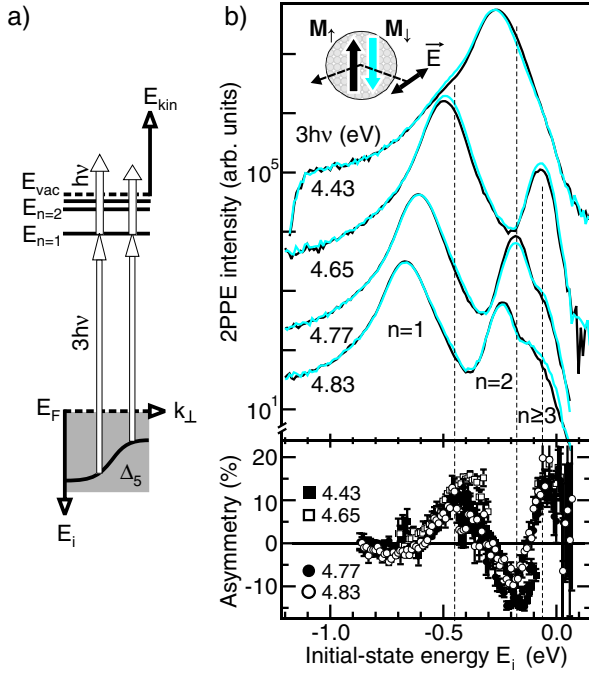
FIG. 1 (color online). (a) Schematic of the 2PPE experiment. (b) Dependence of the spin-averaged 2PPE intensity on the in-plane magnetization of the cobalt film ($\mathbf{M}_\uparrow$ vs $\mathbf{M}_\downarrow$) for p-polarized pump pulses ($3h\nu$). The spectra are plotted on an initial energy scale. The asymmetry A in the lower panel was extracted where intensity is resonantly enhanced by the IPS. Dashed lines mark the position of the maxima of A.

Figure 1(b) presents energy-resolved 2PPE spectra recorded in normal emission, which probes the Δ direction of fcc cobalt. Note that the ordinate axis is logarithmic; the abscissa refers to the initial-state energy E_i below E_F, which means that the peaks of the IPS shift to lower energy with increasing photon energy. Depending on the photon energy the pump pulse resonantly populates the $n = 1$, $n = 2$, and $n \geq 3$ IPS, which converge towards E_{vac} in a Rydberg-like series ($E_n \propto 1/n^2$). Most noticeably, the 2PPE intensity differs for opposite magnetization direction. Because reversal of the uniaxial vector of magnetization $\mathbf{M}$ corresponds to a reflection at the plane defined by the magnetization vector and surface normal, the experimental geometry $\mathbf{M}_\uparrow$ vs $\mathbf{M}_\downarrow$ is inequivalent for p-polarized pump-pulses [cf. inset in Fig. 1(b)] [15]. As expected, we do not observe dichroic contrast for s-polarized pump light (not shown). Figure 1(b) (lower panel) summarizes the normalized dichroic asymmetry of the photoelectron current $A = [I(\mathbf{M}_\uparrow) - I(\mathbf{M}_\downarrow)]/[I(\mathbf{M}_\uparrow) + I(\mathbf{M}_\downarrow)]$. We observe a sizeable asymmetry A of up to 20%. Plotting the data on the initial-state energy scale proves that the asymmetry occurs at fixed E_i and thus reflects a property of the initial valence states.

The time-resolved measurements depicted in Fig. 2 (i) corroborate that the MLD is an initial-state effect
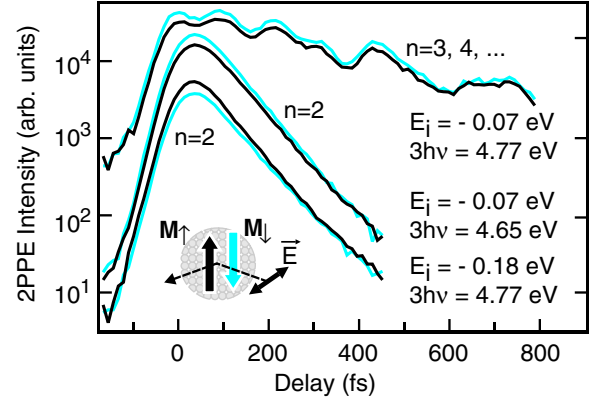

FIG. 2 (color online). Time-resolved measurements of the dichroic decay of the $n = 2$ and $n \geq 3$ IPS. Quantum beats occur among the coherently excited higher states [16].

and (ii) pinpoint their spin character as minority bands. (i) The lower two data traces show the population decay of the $n = 2$ state but have been recorded at distinct initial-state energies E_i. In both cases the spin-averaged decay rate depends on the magnetization direction, but the measurements reveal reversed slopes; i.e., the gray curve is steeper than the black curve for $E_i = -0.07$ eV and vice versa for $E_i = -0.18$ eV. As we probe the same intermediate state, again this must reflect initial-state properties. Likewise the spectra recorded at $E_i = -0.07$ show the same trend, independent of whether we populate the $n = 2$ or the longer-living $n \geq 3$ IPS [10,11,16]. (ii) Naturally, the lifetime of an electronic state has to be independent of the magnetization direction. It is, however, *spin* dependent; electrons excited to minority IPS decay faster than those excited to majority states. For the $3d$ ferromagnets this is due to the larger available phase space for minority electrons in inelastic decay [17,18]. Hence, the apparently dichroic lifetimes follow from the combination of spin-selective excitation which depends on the magnetization direction and the spin-dependent lifetimes. In all the time-resolved measurements the data curves converge at large pump-probe delay, where the decay is dominated by the longer-living majority electrons. If the number of excited *majority* electrons were dependent on the magnetization direction, the time-resolved measurements would diverge rather than converge. Consequently, the dichroic decay reflects dichroic population out of initial-state bands with primarily *minority* character located at energies 0.07 and 0.18 eV below E_F.

The spin-resolved 2PPE spectra in Fig. 3(a) allow us to further unravel the initial-state properties [19]. The spin-splitting of the IPS ($\propto n^{-3}$) reflects the exchange splitting of the bulk bands [10,18]. Concentrating on the spin-dependence of the 2PPE photocurrent it becomes obvious that all the dichroic effects are caused by a change in minority count rate (emphasized by dashed horizontal lines). Figure 3(b) summarizes the spin polarization of
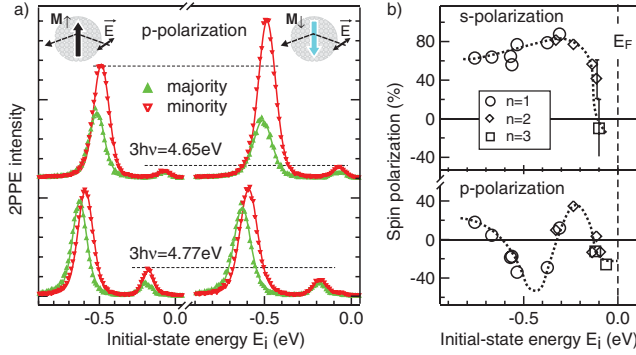
FIG. 3 (color). (a) Spin- and energy-resolved 2PPE data. Red down triangles and green up triangles denote minority and majority electrons. The left (right) panel is recorded for magnetization up $\mathbf{M}_\uparrow$ (down $\mathbf{M}_\downarrow$). (b) Spin-polarization of the IPS for s- and p-polarized pump pulses. Dashed lines are a guide to the eye.

the IPS $(I_{maj} - I_{min})/(I_{maj} + I_{min})$ derived at various photon energies for s- and p-polarized pump pulses, where $I_{maj(min)} = [I_{maj(min)}(\mathbf{M}_\uparrow) + I_{maj(min)}(\mathbf{M}_\downarrow)]/2$. In the following we connect this characteristic spin polarization and dichroism with the fcc cobalt band structure [20].

We calculated the band structure plotted along the main symmetry directions in Fig. 4 within the framework of the spin-polarized fully relativistic Korringa-Kohn-Rostoker multiple-scattering theory [21]. To account properly for electronic correlations beyond the local spin-density approximation (LSDA) [22] we have introduced a general, complex, and energy-dependent self-energy resulting from dynamical mean field theory (DMFT) via a self-consistent LSDA-DMFT calculation [21,23]. Since some part of the correlation effects are included already in LSDA the self-energy is corrected via a self-consistent LSDA-DMFT calculation [23] considering orbital averaged double-counting as described in Ref. [24]. The effective
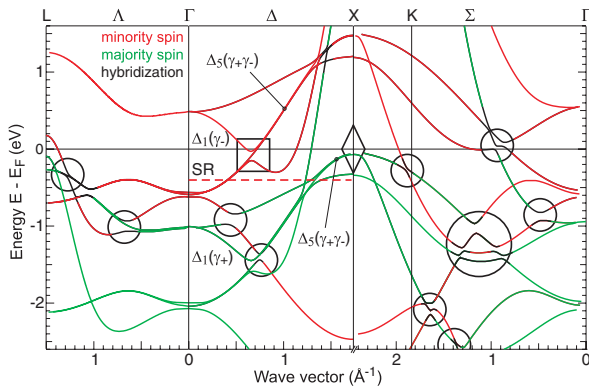

FIG. 4 (color). Spin-polarized fully relativistic band structure calculation of fcc cobalt. Off the hybridization points (square, circles) majority and minority spin bands are colored green and red. The minority-surface resonance experimentally found at −0.45 eV is indicated by the dashed line labeled SR [29].

Coulomb interaction is parametrized by $U = 2.0$ eV and $J = 0.9$ eV. Because of the simultaneous occurrence of spin-orbit coupling and exchange splitting, treated on equal footing in our fully relativistic theory, majority and minority bands hybridize and thus the spin character is no longer well defined. In addition the modified real part of the self-energy acts as a nonlocal, spin- and energy-dependent potential on the various d bands. This changes their dispersion and noticeably increases the exchange splitting with respect to plain LSDA. To identify the spin character of the bands away from the hybridization points we also calculated majority and minority bands separately. In Fig. 4 the relevant bands along the Δ direction are labeled in terms of the nonrelativistic C_{4v} point group $(\Delta_{1,5}^{\uparrow,\downarrow})$ and the relativistic double group $(\gamma_\pm)$. The total-symmetric minority IPS on Co(001) belong to the $\Delta_1^\downarrow$ representation, which reduces to γ_- for the relativistic case. As surface states their energy is independent of perpendicular momentum $k_\perp$. In Ref. [25] it is pointed out that from the initial states along the Δ direction dominantly bulk states at X will contribute to the dipole transition between initial and intermediate states. According to the dipole selection rules we only probe initial states with $\Delta_5^{\uparrow,\downarrow}$ symmetry for s-polarized light [26]. In combination, this explains the spin polarization of up to 80% for s-polarized pump pulses shown in the top panel of Fig. 3(b): the IPS are mainly populated from the majority Δ_5 bulk band close to X. At 100 meV below E_F the spin polarization abruptly drops to negative values. As marked by a diamond in Fig. 4 this must coincide with the top of the majority Δ_5 band at the X point. In our calculation the self-energy correction has been adjusted in order to match this value. All other bands and, in particular, the hybridization point of the $\Delta_1^\downarrow$ and $\Delta_5^\downarrow$ minority bands (square in Fig. 4) follow self-consistently.

Taking spin-orbit coupling into account spin and spatial quantum numbers can no longer be treated independently. This relativistic situation reduces the symmetry of the system and hence the number of representations. The pertinent symmetry class is the double group $\gamma_\pm$, i.e., the product of the C_{4v} point group with the SU(2) group of spin space. An analytical expression for the photocurrent under our experimental conditions can be found in Refs. [15,27] and is reproduced here for convenience:

$$\begin{aligned}
I^\pm = &\sin^2\vartheta(|\mathcal{M}_{1++}|^2 + |\mathcal{M}_{1--}|^2) \\
&+ \cos^2\vartheta(|\mathcal{M}_{5++}|^2 + |\mathcal{M}_{5--}|^2) \\
&\pm \sin\vartheta\cos\vartheta\,\mathrm{Im}(\mathcal{M}_{1++}^*\mathcal{M}_{5++} - \mathcal{M}_{1--}^*\mathcal{M}_{5--}). \quad (1)
\end{aligned}$$

The $\pm$ superscript stands for $\mathbf{M}_\uparrow$ and $\mathbf{M}_\downarrow$ and ϑ denotes the angle between incident light and surface normal. The last term of Eq. (1) is the source for the dichroism. $\mathcal{M}_{1--}^*$ and $\mathcal{M}_{5--}$ denote the optical matrix elements for a transition from γ_- initial bands with Δ_1 and Δ_5 single group representation to a γ_- state. Since the minority IPS have γ_-

symmetry and we have established that only these states show dichroism, only the term $\mathcal{M}_{1--}^{*}\mathcal{M}_{5--}$ is of relevance for our experiment. We must therefore conclude that also the initial states responsible for the observed dichroism have γ_{-} symmetry. We attribute the dichroic features centered at 70 and 180 meV below E_F to the avoided crossing of the $\Delta_1^{\downarrow}$ and $\Delta_5^{\downarrow}$ minority bands. The derived spin-orbit splitting of $\Delta E = 110 \pm 20$ meV and the position close below E_F are in excellent agreement with our band structure calculation (square in Fig. 4, $\Delta E = 120$ meV). The sign of the asymmetry agrees with the calculation in Ref. [28]. Moreover, we provide the experimental proof for the predicted spin and spatial character of the initial valence states.

While the two dichroic features close to E_F are related to bulk bands, we assign the broad positive dichroic structure around $E_i = -0.45$ eV to a minority-surface resonance of $\Delta_1^{\downarrow}$ symmetry (dashed line in Fig. 4). This resonance manifests in the strong dip of the spin polarization observed only for p-polarized pump pulses in Fig. 3(b). The surface resonance has been identified in spin-resolved valence-band photoemission and is confirmed by calculations [29]. Upon spin-orbit coupling it can hybridize with the $\Delta_5^{\downarrow}$ minority bulk band.

Though spin-orbit coupling is in effect throughout the band structure, wave functions are still clearly spin polarized away from the hybridization points. At these hot spots, however, this is no longer true and an electron scattered close to a hot spot has a very high spin-flip probability. We demonstrate here that the hybridization point along the Δ direction is due to a crossing of minority bands. While it is not an obvious spin hot spot, spin-orbit coupling is still strongly enhanced and electron scattering with large momentum transfer may very well support spin-flip processes. More obvious, two bands with different spin in the nonrelativistic limit show an admixture of spin components in the electron wave function in the presence of spin-orbit coupling. Thus our band structure calculation, which is in excellent agreement with the measurement, predicts a second spin hot spot close to E_F along the Σ direction. It therewith substantiates the proposed underlying mechanism of ultrafast demagnetization in fcc cobalt [6,9].

In conclusion, spin-resolved 2PPE in combination with magnetic linear dichroism on Co(001) allows us to pinpoint spin-orbit hybridization points in ferromagnets. We resolve a spin-orbit splitting of 110 meV between minority valence bands with Δ_1 and Δ_5 spatial parts close below the Fermi level. Excellent agreement is achieved with fully relativistic band structure calculations which predict a second spin hot spot along the Σ direction of fcc cobalt. Excited holes can scatter at these hybridization points, where the high spin-flip probability facilitates demagnetization on a femtosecond time scale.

*Corresponding author: weinelt@mbi-berlin.de
[1] P. Bruno, Phys. Rev. B **39**, 865 (1989).
[2] J. Smit, Physica (Amsterdam) **17**, 612 (1951).
[3] A. Vaterlaus *et al.*, Phys. Rev. B **46**, 5280 (1992).
[4] E. Beaurepaire, J.-C. Merle, A. Daunois, and J.-Y. Bigot, Phys. Rev. Lett. **76**, 4250 (1996).
[5] B. Hillebrands and K. Ounadjela, *Spin Dynamics in Confined Magnetic Structures I & II*, Topics in Applied Physics (Springer, New York, 2002).
[6] B. Koopmans, J. J. M. Ruigrok, F. D. Longa, and W. J. M. de Jonge, Phys. Rev. Lett. **95**, 267207 (2005).
[7] J. Kirschner, Phys. Rev. Lett. **55**, 973 (1985).
[8] J. Fabian and S. D. Sarma, Phys. Rev. Lett. **81**, 5624 (1998); **83**, 1211 (1999).
[9] M. Cinchetti *et al.*, Phys. Rev. Lett. **97**, 177201 (2006).
[10] M. Weinelt, A. B. Schmidt, M. Pickel, and M. Donath, Prog. Surf. Sci. **82**, 388 (2007).
[11] P. M. Echenique *et al.*, Surf. Sci. Rep. **52**, 219 (2004).
[12] J. Kirschner and R. Feder, Phys. Rev. Lett. **42**, 1008 (1979); D. H. Yu *et al.*, Surf. Sci. **601**, 5803 (2007).
[13] The preparation results in a sharp unmixed interface with equivalent electronic structure for 6 and 7 ML Co [14].
[14] D. H. Yu, M. Donath, J. Braun, and G. Rangelov, Phys. Rev. B **68**, 155415 (2003).
[15] W. Kuch and C. M. Schneider, Rep. Prog. Phys. **64**, 147 (2001).
[16] U. Höfer *et al.*, Science **277**, 1480 (1997).
[17] F. Passek, M. Donath, K. Ertl, and V. Dose, Phys. Rev. Lett. **75**, 2746 (1995); M. Aeschlimann *et al.*, Phys. Rev. Lett. **79**, 5158 (1997).
[18] A. B. Schmidt *et al.*, Phys. Rev. Lett. **95**, 107402 (2005).
[19] A. Winkelmann *et al.*, Phys. Rev. Lett. **98**, 226601 (2007).
[20] C. M. Schneider *et al.*, J. Phys. Condens. Matter **3**, 4349 (1991); O. Andreyev *et al.*, Phys. Rev. B **74**, 195416 (2006).
[21] H. Ebert, in *Electronic Structure and Physical Properties of Solids*, edited by H. Dreyssé (Springer, Berlin, 2000); J. Minár *et al.*, Phys. Rev. B **72**, 045125 (2005).
[22] P. Hohenberg and W. Kohn, Phys. Rev. **136**, B864 (1964); W. Kohn and L. J. Sham, Phys. Rev. **140**, A1133 (1965); R. O. Jones and O. Gunnarsson, Rev. Mod. Phys. **61**, 689 (1989).
[23] G. Kotliar and D. Vollhardt, Phys. Today **57**, No. 3, 53 (2004); A. Georges *et al.*, Rev. Mod. Phys. **68**, 13 (1996).
[24] J. Braun *et al.*, Phys. Rev. Lett. **97**, 227601 (2006).
[25] W. Wallauer and Th. Fauster, Phys. Rev. B **54**, 5086 (1996).
[26] W. Eberhardt and E. W. Plummer, Phys. Rev. B **21**, 3245 (1980).
[27] J. Henk, T. Scheunemann, S. V. Halilov, and R. Feder, J. Phys. Condens. Matter **8**, 47 (1996).
[28] A. Fanelsa, E. Kisker, J. Henk, and R. Feder, Phys. Rev. B **54**, 2922 (1996).
[29] A. B. Schmidt *et al.*, J. Phys. D (to be published); K. Miyamoto *et al.*, Phys. Rev. B (to be published).